J. Membrane Biol. 181, 137–148 (2001)
DOI: 10.1007/s00232-001-0017-1

The Journal of
Membrane
Biology

Intracellular Domains of Mouse Connexin26 and -30 Affect Diffusional and Electrical Properties of Gap Junction Channels

D. Manthey[1,*], K. Banach[2], T. Desplantez[2], C.G. Lee[3,4], C.A. Kozak[3], O. Traub[1], R. Weingart[2], K. Willecke[1]
[1]Institut für Genetik, Abt. Molekulargenetik, Universität Bonn, Römerstr. 164, 53117 Bonn, Germany
[2]Dept. of Physiology, University of Bern, Bühlplatz 5, 3012 Bern, Switzerland
[3]National Inst. of Allergy and Infectious Diseases, 9000 Rockville Pike, BLDG. 4, Room 329, Bethesda, MD 20892, USA
[4]Department of Internal Medicine, Yale University School of Medicine, New Haven, CT 06520, USA

Received: 26 July 2000/Revised: 15 February 2001

Abstract. To evaluate the influence of intracellular domains of connexin (Cx) on channel transfer properties, we analyzed mouse connexin (Cx) Cx26 and Cx30, which show the most similar amino acid sequence identities within the family of gap junction proteins. These connexin genes are tightly linked on mouse chromosome 14. Functional studies were performed on transfected HeLa cells stably expressing both mouse connexins. When we examined homotypic intercellular transfer of microinjected neurobiotin and Lucifer yellow, we found that gap junctions in Cx30-transfected cells, in contrast to Cx26 cells, were impermeable to Lucifer yellow. Furthermore, we observed heterotypic transfer of neurobiotin between Cx30-transfectants and HeLa cells expressing mouse Cx30.3, Cx40, Cx43 or Cx45, but not between Cx26 transfectants and HeLa cells of the latter group. The main differences in amino acid sequence between Cx26 and Cx30 are located in the presumptive cytoplasmic loop and C-terminal region of these integral membrane proteins. By exchanging one or both of these domains, using PCR-based mutagenesis, we constructed Cx26/30 chimeric cDNAs, which were also expressed in HeLa cells after transfection. Homotypic intercellular transfer of injected Lucifer yellow was observed exclusively with those chimeric constructs that coded for both cytoplasmic domains of Cx26 in the Cx30 backbone polypeptide chain. In contrast, cells transfected with a construct that coded for the Cx26 backbone with the Cx30 cytoplasmic loop and C-terminal region did not show transfer of Lucifer yellow. Thus, Lucifer yellow transfer can be conferred onto chimeric Cx30 channels by exchanging the cytoplasmic loop and the C-terminal region of these connexins. In turn, the cytoplasmic loop and C-terminal domain of Cx30 prevent Lucifer yellow transfer when swapped with the corresponding domains of Cx26. In chimeric Cx30/Cx26 channels where the cytoplasmic loop and C-terminal domains had been exchanged, the unitary channel conductance was intermediate between those of the parental channels. Moreover, the voltage sensitivity was slightly reduced. This suggests that these cytoplasmic domains interfere directly or indirectly with the diffusivity, the conductance and voltage gating of the channels.

Key words: Lucifer yellow — Neurobiotin — Electrophysiology — Chimeric connexins — Structure-function relationship

Introduction

Gap junction channels in the mouse consist of at least 16 different protein subunits, called connexins (Cx) (cf. Bruzzone et al., 1996; Simon and Goodenough, 1998; Condorelli et al., 1998; Söhl et al., 1998; Manthey et al., 1999; Teubner et al., 2001). Six connexin subunits can assemble into a hemichannel (connexon). Functional gap junction channels are formed by docking of two hemichannels in contacting membranes of apposed cells. The channels form aqueous pores which are permeable to ions and small molecules (<1 kDa) such as metabolites or second messengers. Gap junction mediated cell-to-cell communication has been implicated in the intercellular transmission of electrical signals in cardiac and neuronal tissues (cf. Bennett, 1997), in the regulation of the early development (Davies et al., 1996; Dahl et al., 1996a; Delorme et al., 1997; Nadarajah et al., 1997; Strata et al., 1998), in the cellular growth control and the

* *Present address:* Max Planck Institute of Psychiatry, Kraepelinstr. 2, 80804 München, Germany

Correspondence to: K. Willecke

suppression of tumorigenesis (Yamasaki & Naus, 1996; Temme et al., 1997).

All members of the connexin family investigated share the same membrane topology. Based on hydropathy plots, limited proteolysis of membrane-embedded connexins and site-directed antibodies to Cx32, Cx43 and Cx26 (Milks et al., 1988; Laird & Revel, 1990; Zhang & Nicholson, 1994), it was concluded that connexins span the plasma membrane four times (M1–M4) and form two extracellular loops (E1, E2) and three cytoplasmic regions (amino- [C1], carboxyl-terminal region [C3], cytoplasmic loop [C2]). The nomenclature of connexins is deduced from the predicted molecular mass of connexins (Beyer et al., 1988) or the use of Greek letters for different connexin subgroups, based on similarities in the cytoplasmic loop (Gimlich, Kumar & Gilula, 1990; Goodenough, Goliger & Paul, 1996; Söhl et al., 1998). Within the connexin gene family, major differences in sequence and length were found in the cytoplasmic loop and the carboxy-terminal region. It seems reasonable to assume that functional differences among connexin channels may depend on structural differences in the cytoplasmic domains. The establishment of gap junctional communication depends on two distinct properties, the docking of two hemichannels and the gating of each hemichannel. The docking of two hemichannels is determined by the extracellular loops (Haubrich et al., 1996), especially domain E2 (Zhu, Cinbotaru & Nicholson, 1998). Gap junction channels are designated as homotypic when the hemichannels contributed by each cell are composed of the same type of connexin, or as heterotypic when each hemichannel is formed by a different type of connexin. The pH-dependent gating of Cx43 channels has been shown to depend on the interaction between C2 and C3. In order to explain this effect, Delmar et al. (1998) suggested a "particle-receptor" model analogous to the "ball-on-a-chain" model of voltage-dependent K^+ channels (Hoshi et al., 1990; Marten & Hoshi, 1997). In this model, the C3 region acts as "particle" and the C2 loop as "receptor".

Connexin channels differ in their permeability to dye and tracer molecules (Elfgang et al., 1995) as well as metabolites (Goldberg, Bechberger & Naus, 1995). To check whether the cytoplasmic domains contribute to the diffusional properties, we have investigated Cx26 and Cx30 channels. It has been reported that the amino acid sequences of Cx26 and Cx30 share the highest sequence identity (77%; Dahl et al., 1996b) among known connexins. Both connexin genes had been assigned to mouse chromosome 14 but show different patterns of expression (Dahl et al., 1996b). The corresponding gap junction channels exhibit different single channel conductances (Cx26: 100 pS; Valiunas et al., 1999b; Cx30: 180 pS; Valiunas et al., 1999a).

Here we report that these genes are tightly linked on mouse chromosome 14. For the evaluation of dye diffusion through homotypic and heterotypic Cx26 and Cx30 channels, the coding region of this mouse gene was expressed in human HeLa cells and the transfectants were analyzed by microinjection of neurobiotin and Lucifer yellow. Whereas Cx26 cells (Elfgang et al., 1995) showed intercellular transfer of Lucifer yellow, Cx30 cells did not. This difference is likely to be caused by the different amino acid composition. The largest differences in the sequence of amino acid residues are located in C2 and C3 of these connexins. To characterize the protein domains possibly responsible for these differences in dye diffusion, we isolated Cx26/30 chimeric constructs in which DNA regions coding for C2, C3 or both were exchanged. After expression of these chimeric constructs in HeLa cells, we analyzed the gap junction channels in the transfected cell clones by dye transfer and electrophysiological measurements. We found that the C2 and C3 regions of Cx26 and Cx30 affect the dye transfer, the conductance and voltage sensitivity of the channels.

Materials and Methods

Genetic Mapping

Connexin genes were mapped by analysis of two sets of mouse crosses: (*NFS/N* or *C58/J* × *M. musculus*) × *M. musculus* (Kozak et al., 1990) and (*NFS/N* × *M. spretus*) × *M. spretus* or *C58/J* (Adamson Silver & Kozak, 1991). Progeny of these crosses was typed for over 1,200 markers including the chromosome 14 loci *Np* (nucleoside phosphorylase), *Tcra* (T cell receptor alpha), *Blk* (B cell tyrosine kinase), *sys* (symplastic spermatids), *Int6-ps5* (mammary tumor virus integration 6-pseudogene 5) and *Gnbl-rs3* (guanine nucleotide binding protein 1-related sequence 3), as described previously (Kozak et al., 1991; Miyazaki et al., 1995).

Construction and Cloning of Connexins and Chimeric Connexins

The chimeric connexins were constructed by PCR-amplification of parts of the coding region of mouse Cx26 and -30 (Willecke et al., 1991 [Genbank/EMBL/DDBJ accession No. M81444]; Dahl et al., 1996b [Genbank/EMBL/DDBJ accession No. Z70023]). For the PCR, primers were selected or designed to include restriction sites. Before ligation of PCR fragments to complete chimeric connexins, the fragments were digested with endonucleases to generate "sticky ends" for ligation.

The DNA amplification was performed with PWO DNA Polymerase (Eurogentec, Seraing, Belgium) according to the manufacturer's protocol. Amplification reactions were carried out in a PTC-100 Thermal Cycler (MJ Research, Watertown, MA) (3 min at 94°C; 30 cycles [1 min at 60°C, 2 min at 72°C, 3 min 94°C]; 5 min at 72°C). After cloning of the constructs into the expression vector pBluescript II SK+ (Stratagene, La Jolla, CA) each construct was fully sequenced in both directions.

To generate the Cx26∗30C3 construct, a 665 bp fragment of mouse Cx26 was amplified with the sense 5′ GTCTTCTCCAGTGC-

CAAGGATCCAGAGGAC 3′ and antisense 5′ CGAACAAATAG-CAGAGCTCTGTGATATTTAGC 3′ primers. By using these primers and genomic Cx26 DNA (Hennemann et al., 1992) as template, a fragment from position −33 to −632 was generated, coding for the N-terminus until the beginning of the presumptive cytoplasmic tail of Cx26. During PCR, restriction sites for BamHI at the 5′ end and for SacI at the 3′ end were generated. A second PCR using genomic mouse Cx30 DNA as template and the sense 5′ GCTCAATGTGGC-CGAGCTCTGTTACCTGCTGC 3′ as well as antisense 5′ CT-TATATTGTGTATGAAGAGCTCAGGTGTTC 3′ primers, yielded a 348 bp fragment (postition 621 to 969) coding for a part of transmembrane region M4 and the cytoplamic tail of mouse Cx30 generating SacI restriction sites on both ends. For ligation and cloning of the chimeric Cx26∗30C3 construct, the Cx26 fragment was digested with SacI and BamHI, and the Cx30 fragments were digested with SacI. Both fragments were ligated in the BamHI/SacI linearized vector pBluescript II SK+. Afterwards, the Cx26∗30C3 insert was cloned in the expression vector pBEHpac18 (Horst, Harth & Hasilik, 1991; Elfgang et al., 1995) by digestion with the restriction endonucleases BssHII after blunting the DNA ends with Klenow polymerase as well as Asp718 and ligation in XbaI (after blunting the DNA ends) in Asp718 linearized pBEHpac18 DNA. The nomenclature of these and the following Cx26/Cx30 chimeric constructs is illustrated schematically in Fig. 3.

The chimeric Cx30∗26C3 construct was generated by amplification of a 667 bp Cx30 fragment (primers: sense 5′ GTATGTT-TAAGAATAAGCTTGCACGATGGACTG 3′, antisense 5′ GCAG-CAGGTAACAGAGCTCGGCCACATTGA 3′) with a HindIII restriction site at the 5′ end and a SacI cleavage site at the 3′ end. This fragment contained the coding region of mouse Cx30 from the N-terminus to the middle of the M4 domain. The Cx26C3 domain was constructed by using 5′ GCTAAATATCACAGAGCTCTGCTATTT-GTTCG 3′ as sense and 5′ CGCCAGTGATGAATACAATAG-GTGGGCCCTC 3′ as antisense primer. The resulting 785 bp fragment (position 611 to 1396) contained an internal SacI site (position 758) and a SacI site at the 5′ end. The Cx30 fragment was digested with SacI and HindIII, and the Cx26 fragment only with SacI. Both fragments were ligated in HindIII/SacI linearized vector pBluescript II SK+. The Cx30∗26C3 fragment was isolated by digestion with BssHII and HindIII, both ends were blunted by treatment with Klenow-Polymerase (BM) and then ligated in XbaI (after blunting the DNA ends) linearized expression vector pBEHpac18.

The Cx26∗30C2 construct was generated by fusion of three PCR amplified fragments. The first fragment reached from the N-terminal part to the end of the M2 region of Cx26 (325 bp, position −33 to −291) and contained a novel BamHI site at the 5′ end and an NsiI site at the 3′ end (sense primer: 5′ GTCTTCTCCAGTGCCAAGGATCCAGAG-GAC 3′, antisense primer: 5′ GGTAGGCCACATGCATAGCTAC-CAGGAGGGCTG 3′). For the Cx30 C2 part of the construct, a 139 bp fragment (position 269 to 408) was amplified (sense 5′ CAGCCCT-GTTGGTGGCCATGCATGTGGCCTAC 3′, antisense 5′ CCACAG GGAGCCATCGATGCGCACCTTCTGCCG 3′) with an artificial NsiI site at the 5′ end and an artificial ClaI site at the 3′ end. The third part, a 1052 bp fragment containing the Cx26 sequence from the M3 domain to the end of the C3 domain, was generated by using the sense primer (5′ CAAAACCCAGAAGGTCCGTATCGATGGGTCCCTGTG 3′) and antisense primer (5′ CGCCAGTGATGAATACAATAG-GTGGGCCCTC 3′). The fragment contained at the 5′ end an artificial ClaI site and an internal SacI site (position 758) for ligation and merging of the Cx26∗30C2 construct. The three fragments were digested with suitable restriction endonucleases and ligated together with BamHI/SacI linearized vector DNA of pBluescript SKII+ (Stratagene) to yield the chimeric construct. For transfection, the construct was digested with BssHII, the ends were blunted with Klenow polymerase (Roche, Mannheim, Germany) and then digested with Asp718. The Asp718/BssHII (blunt) fragment was ligated into Asp718/XbaI (after blunting the DNA ends)-linearized vector pBEHpac18.

The Cx30∗26C2 construct was generated by a similar procedure as the Cx26∗30C2 construct. The part coding for the N-terminal region to the M2 region of Cx30 was amplified by using sense primer 5′ GTATGTTTAAGAATAAGCTTGCACGATGGACTG 3′ and antisense primer 5′ GTAGGCCACATGCATGGCCACCAACA GGGCTGG 3′. During the PCR reaction, a 315 bp fragment (position −25 to 291) with an artificial HindIII site at the 5′ end and an artificial NsiI site at 3′ end was generated. The C2 region of Cx26 was constructed by PCR with the sense primer 5′ CAGCCCTCCTGGTAGC-TATGCATGTGGCCTAC 3′ and antisense primer 5′ CCACAGG-GACCCATCGATACGGACCTTCTGCGTTTTG 3′. This 104 bp fragment (position 258-398) contained an artificial NsiI site at the 5′ end and an artificial ClaI site at the 3′ end. The third subfragment of the construct coded for the M3 domain to the end of the C3 domain of the Cx30 gene (597 bp). It was amplified by using sense primer 5′-CAAACGGCAGAAGGTGCGCATCGATGGCTCCCTGTG-3′ and antisense primer 5′-CTTATATTGTGTATGAAGAGCTCAGGT-GTTC-3′ with an artificial ClaI site at the 5′ end and an artificial SacI site at the 3′ end. The three fragments were digested with the corresponding restriction endonucleases and ligated into HindIII/SacI linearized Vector pBluescript II SK+. For transfection, the chimeric construct was ligated after BssHII/HindIII digestion and Klenow treatment into DNA of XbaI (blunted DNA ends) linearized expression vector pBEHpac18.

For construction of the C2,C3 double substituted connexins, the previously described single exchange chimeric constructs were used as templates. For the Cx26∗30C2,C3 chimeric connexin, the Cx26∗30C2 construct was partially digested with ClaI/BssHII in order to remove a fragment corresponding to M3 until the 3′ non-translated region. This part was replaced from the analogous region of the Cx26∗30C3 construct. It was generated by PCR with the sense primer 5-CAAAAC-CCAGAAGGTCCGTATCGATGGGTCCCTGTG-3′ and the M13 reverse primer (Amersham, Braunschweig, Germany) as reverse primer. The fragment was digested with BssHII/ClaI and ligated in the BssHII/ClaI site of the Cx26∗20C2/pBluescript SKII+. The Cx26∗30C2,C3 fragment was ligated in the expression vector pBEHpac18 as described for the Cx26∗30C2 construct.

The Cx30∗26C2,C3 chimeric construct was generated as described above for the Cx26∗30C2,C3 construct. In a partial digestion of Cx30∗26C2 DNA with BssHII/ClaI, the subfragment corresponding to the M3 domain (coding for the third transmembrane region) until the 3′ nontranslated region of Cx30 was removed and replaced from the analogous region of the Cx30∗26C3 construct. This fragment was generated by amplification with the sense primer 5′-CAAAC GGCAGAAGGTGCGCATCGATGGCTCCCTGTG-3′ and “M13 reverse primer” (Amersham).

With the chimeric Cx26∗26C3 construct, a Cx26 wild-type construct was generated to serve as internal control of the construction strategy. For this purpose, the 30C3 fragment of the Cx26∗30C3 construct was removed by SacI digestion and replaced by the Cx26C3 SacI fragment of the Cx30∗26C3 chimeric construct.

Cells and Culture Conditions

Experiments were performed with HeLa cells (Human cervix carcinoma cells, ATCC CCL29; cf. Eckert et al., 1993). These cells and their transfectants were grown in Dulbecco’s modified Eagles medium (Gibco BRL, Eggenstein, Germany), supplemented with 10% fetal calf serum (Gibco BRL), 100 μg/ml streptomycin and 100 μg/ml penicillin (cf. Hennemann et al., 1992). The medium for the HeLa transfectants

contained in addition 1 μg/ml puromycin (Sigma, St. Louis, MO). The cells were passaged weekly, diluted 1:10 and maintained in a 37°C incubator with a moist atmosphere of 5% CO_2/95% air.

Transfection

Cloning, construction and transfection of the HeLa-Cx26 cell clone E were described by Elfgang et al. (1995). The isolation of mouse Cx30-transfected HeLa cells was described by Valunias et al. (1999a). For designation of chimeric connexin constructs we used the same nomenclature as described in Haubrich et al. (1996). For transfection of HeLa cells with the Cx26∗30C3, Cx30∗26C3, Cx26∗30C2 chimeric constructs, 20 μg plasmid-DNA were used for the calcium phosphate transfection protocol of Graham and van der Ebb (1973) (Sambrook, Fritsch & Maniatis, 1989). The chimeric connexin constructs Cx30∗26C2, Cx26∗30C2,C3 and Cx30∗26C2,C3 were transfected in HeLa cells using the commercial lipofection reagent Tfx-20 (Promega, Madison, WI) according to the manufacturers' protocol. Forty-eight hours after incubation with the DNA/calcium phosphate precipitate or DNA/lipofection solution, 1 μg/ml puromycin was added to the medium. Clones were picked after 3 weeks and grown under selective conditions. Expression of connexin mRNAs was checked by Northern blot analysis.

Microinjection of Tracers

Glass micropipettes were pulled from capillary glass (WPI Inc., Berlin, Germany) with a horizontal pipette puller (PD-5, Narishige, Tokyo, Japan) and backfilled with tracer solution. Tracers were injected iontophoretically (Iontophoresis Programmer Model 160; WPI Inc.). Dye transfer was examined, using an inverse microscope (IM35; Zeiss, Oberkochen, Germany) with fluorescent illumination (HBO100; Zeiss). During injection, cell culture dishes were kept on a heated block at 37°C.

Lucifer yellow (LY) CH (Molecular Probes, Eugene, OR) as 4% (w/v) in 1 M LiCl was injected by applying negative voltage for 10 sec (I = 20 nA). Cell-to-cell transfer was evaluated by fluorescent microscopy (Zeiss IM-35, filter set 9) 5 min after dye injection. Neurobiotin (*N*-2(2-aminoethyl)-biotinamide hydrochloride; Vector Lab, Burlingame, CA) and rhodamine 3-isothiocyanate dextran 10S (Sigma) at concentrations of 6% and 0.4% (w/v) in 0.1 M Tris-Cl (pH 7.6) were injected iontophoretically by application of positive voltage for 10 sec (I = 20 nA). The transfer of tracer molecules was observed using filter set 15 (Zeiss) in the microscope. Ten min after injection, cells were washed twice with phosphate buffered saline (PBS), fixed for 10 min in 1% glutaraldehyde in PBS, washed twice with PBS, incubated in 2% Triton X100/PBS for 2 hr, washed three times with PBS, incubated with horseradish peroxidase-avidin D diluted 1:1000 in PBS (Vector Lab.), for 90 min, washed three times with PBS, and incubated in 0.05% diaminobenzidine (Sigma)/0.003% hydrogen peroxide solution for 30 sec to 2 min. The staining reaction was stopped by washing three times with PBS. Cell-to-cell transfer was quantified by counting the number of stained neighbouring cells around the injected cell.

For assay of heterotypic coupling, one cell type was prestained with DiI ($DiIC_{18}$ (1,1′-dioctadecyl-3,3,3′,3′-tetramethylindocarbocyanine perchlorate; Molecular Probes) as described by Goldberg et al. (1995) and co-cultivated with a 1,000-fold excess of unstained cells expressing a different connexin gene. DiI-stained cells were identified using filter set 15 (Zeiss). The cells were incubated for 18 hr before microinjection of neurobiotin or Lucifer yellow.

Northern Blot Hybridization

Total RNA from HeLa cells was prepared with the QIA RNeasy Kit, as described by the company (Qiagen, Hilden, Germany) and aliquots of 5 μg were electrophoresed. Northern blots, hybridization at high stringency conditions (55% formamide, 42°C, 5 × SSC), filter washing, and autoradiography were performed as described previously (Willecke et al., 1991). A 590 bp PCR fragment of Cx30 (position 25 to 615) and a 1 kb EcoRI fragment containing the entire coding region of Cx26 were used after denaturation for hybridization analysis.

Immunofluorescence Analysis

Immunolabelling of Cx26, Cx30 and chimeric connexin proteins was performed on cultured HeLa transfectants grown on glass coverslips as described previously (Dermietzel et al., 1984). Cells were incubated with 1:50 diluted rabbit anti-Cx26 (Traub et al., 1989) or rabbit anti-Cx30 (cf. Kunzelmann et al., 1999) for 2 hr at room temperature. Immunosignals were visualized using 1:800 diluted FITC-conjugated goat anti-rabbit IgG (Dianova, Hamburg, Germany) for 1 hr at room temperature. For documentation of fluorescent images, a Zeiss Axiophot microscope and Fuji chrome Provia 400 film were used.

Evaluation of Tracer Transfer

Homotypic transfer of neurobiotin or Lucifer yellow in connexin-transfected HeLa cell clones was carried out by evaluating the spreading of microinjected tracer into cells around the injected cell (cf. Elfgang et al., 1995). For assays of tracer transfer, more than twenty microinjections were carried out in a given type of transfected cell. Homo- and heterotypic transfer was considered to be positive when more than 80 percent of the neighbouring cells were stained by the injected tracer. This procedure excluded negative clones which showed only few and slightly stained neighbouring cells, presumably due to low level of endogenous coupling in wild-type HeLa cells (Elfgang et al., 1995; Cao et al., 1998). The data are presented as means ± SD. Statistical evaluations were done using paired Student's *t*-tests.

Electrophysiology

HeLa cells were seeded onto glass coverslips (~10^4 cells/cm^2) placed in multiwell dishes. Within two days after plating, coverslips with adherent cells were transferred to an experimental chamber superfused with Krebs-Ringer solution (in mM): NaCl 140, KCl 4, $CaCl_2$ 2, $MgCl_2$ 1, glucose 5, pyruvate 2, HEPES 5 (pH 7.4); temperature: 20–23°C. The chamber was mounted on the stage of an inverted microscope equipped with phase-contrast optics. Patch pipettes were pulled from glass capillaries with a horizontal puller (DMZ-Universal; Zeitz-Instrumente, Augsburg, Germany). The pipettes were filled with solution containing (in mM) potassium aspartate 120, NaCl 10, MgATP 5, $MgCl_2$ 1, $CaCl_2$ 1, EGTA 10 (pCa ~8), HEPES 5 (pH 7.2). When filled, the pipettes had resistances of 2–4 MΩ.

Experiments were carried out on pairs of cells using the dual voltage-clamp method in conjunction with tight-seal, whole-cell recording (cf. Valiunas et al., 1999a). Each cell was attached to a patch pipette connected to a separate micromanipulator (WR-88; Narishige Scientific Instrument, Tokyo, Japan) and amplifier (EPC7; List Electronics, Darmstadt, Germany). This approach permitted to control the membrane potential of each cell (V_1, V_2) and measure the currents through both pipettes (I_1, I_2). I_1 and I_2 correspond to the sum of two currents, $I_{m,1} + I_j$ and $I_{m,2} - I_j$ (I_j: gap junction current). Deflections in I_1 and I_2, coincident in time and opposite in polarity, reflect changes in I_j. The conductance of a gap junction, g_j, or a gap junction channel, γ_j, is given by the ratio $I_j/(V_2 - V_1)$. $V_2 - V_1$ corresponds to the voltage across the gap junction, V_j. Voltage and current signals were recorded on FM-tape. For off-line analysis, the current signals were filtered at 1

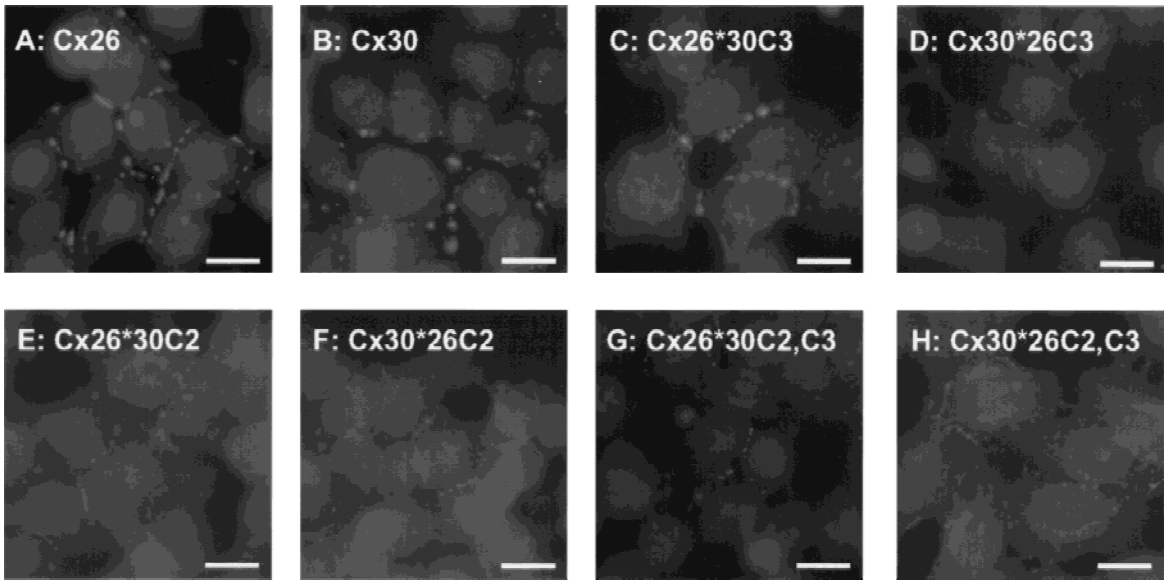

Fig. 1. Immunofluorescence analyses of selected HeLa transfectants after incubation with rabbit Cx26- and Cx30-antibodies and FITC-conjugated goat anti-rabbit IgG. Bar, 25 μm. (*A*) HeLa Cx26 transfectants incubated with anti-Cx26. (*B*) HeLa Cx30 transfectants incubated with anti-Cx30. (*C*) HeLa Cx26∗30C3 transfectants incubated with anti-Cx30. (*D*) HeLa Cx30∗26C3 transfectants incubated with anti-Cx26. (*E*) HeLa Cx26∗30C2 transfectants incubated with anti-Cx26. (*F*) HeLa Cx30∗26C2 transfectants incubated with anti-Cx30. (*G*) HeLa Cx26∗30C2,C3 transfectants incubated with anti-Cx26. (*H*) HeLa Cx30∗26C2,C3 transfectants incubated with anti-Cx26.

kHz (8-pole Bessel, –3 dB) and digitized at 5 kHz with a 12-bit A/D converter. Data acquisition and analyses were done with the software C-Lab (Indec Systems, Capitola, CA). The results are presented as means ± 1 SEM.

Results

Genetic Mapping of Mouse Cx26 and Cx30 Genes

To position these genes on the chromosome, DNAs of the progeny of the *M. spretus* crosses were typed for PstI and ApaI restriction enzyme polymorphisms in the Cx26 and Cx30 sequences, and XbaI and BglII identified variants of the two genes in the *M. m. musculus* crosses. Comparisons with inheritance of other markers previously mapped in these crosses indicated that the Cx26 and Cx30 genes were located at a common site on chromosome 14. No recombinants were identified between Cx30 and Cx26 genes in 187 mice indicating that, at the upper limit of 95% confidence level, these markers are located within 1.59 cM. Gene order and distances in the *M. m. musculus* crosses are as follows: Np,Tcra − 4.0 ± 1.6 − Cx26,Cx30 − 6.0 ± 2.4 − Blk. In the *M. spretus* crosses, linkage is as follows: *Np* − 3.6 ± 1.8 − Cx26, Cx30,Gnb1-rs3 − 3.1 ± 1.8—Int6-ps5. This map location is consistent with the previously described location of Cx26 on this chromosome suggesting that at least 3 connexin genes are clustered at this site (Haefliger et al., 1992; Schwarz et al., 1992; Dahl et al., 1996b).

Functional Analysis of HeLa Cx30 Transfectants

The HeLa Cx30 transfectants together with HeLa wild type cells were characterized by Northern blot hybridization. Three transfectants (clones B, D, E) showed the expected hybridization signal at 1.1 kb, whereas HeLa-Cx30, clone G, yielded a signal at 4.5 kb, presumably due to different transcriptional termination sites of different integrated copies of the inserted plasmid DNA (*data not shown*). As a representative example of our immunofluorescence analysis, Fig. 1 illustrates HeLa-Cx30 clone E cells that express punctate immunofluorescent signals of contact membranes, the typical site of gap junction plaques. The function of gap junction channels established by wild-type and mutated connexins was examined by microinjection of neurobiotin (molecular mass 287 Da, charge +1). The spreading of neurobiotin in the different HeLa-Cx30 transfectants is shown in Fig. 2. HeLa-Cx30-E cells exhibited the highest RNA as well as protein level and most efficient neurobiotin transfer. Transfer of the microinjected dyes, Lucifer yellow (molecular mass 443 Da, charge −2) and calcein (molecular mass 623 Da, charge −4) was not detected among HeLa-Cx30 cells, whereas both dyes could readily permeate Cx26 channels in HeLa-Cx26 cells (Elfgang et al., 1995, and unpublished observations). Because of the relatively low molecular mass of neurobiotin and the observation that the HeLa connexin transfectants, which exhibited increased electrical conductance above background, also showed transfer of neu-

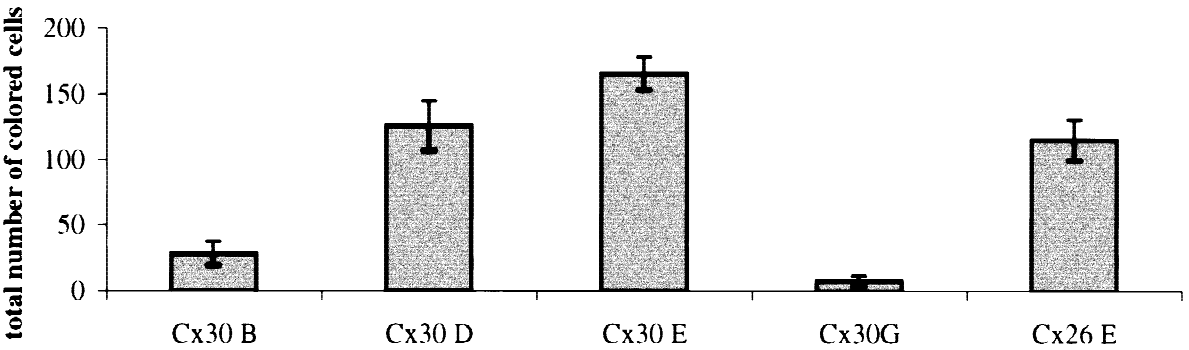

Fig. 2. Homotypic transfer of microinjected neurobiotin in Cx26- and Cx30-transfected HeLa cell clones. The columns represent the mean standard value (mv) of neurobiotin spreading to neighboring cells. The error bars are indicated as ±SD.

robiotin, we assume that the spreading of microinjected neurobiotin is proportional to the number of functional gap junction channels in HeLa-connexin transfectants. In order to confirm that Cx30 channels are not permeable to Lucifer yellow, and to rule out that this was caused by low expression of Cx30 gap junction channels, we compared neurobiotin transfer of HeLa-Cx30 transfectants with HeLa-Cx26 transfectants (Table 1). Although HeLa-Cx26 clone E cells were permeable to Lucifer yellow (Elfgang et al., 1995), these cells showed lower transfer of neurobiotin than the HeLa-Cx30 clones D and E (Fig. 2).

Formation of Heterotypic Gap Junction Channels with HeLa-Cx30 Transfectants

In order to analyze the formation of functional heterotypic gap junctions with HeLa-Cx30 transfectants, we prelabelled one type of transfectant with the inert membrane dye DiI (Goldberg et al., 1995). The labelled cells were cocultured with a 1,000-fold excess of unlabelled transfectants for 18 hr before microinjection of neurobiotin. Table 2 lists functional heterotypic gap junction channels formed with Cx30 hemichannels in comparison to Cx26 hemichannels. Only HeLa-Cx30 but not HeLa-Cx26 cells can form functional heterotypic channels with HeLa cells transfected with Cx30.3, Cx43 or Cx45.

Characterization of Cx26/Cx30 Chimeric Constructs after Transfection into HeLa Cells

We wanted to investigate the influence of the cytoplasmic loop and the C-terminal domains on the properties of chimeric gap junction channels by exchange between Cx26 and Cx30 proteins. The constructions of the domain exchange mutants were performed by cloning of PCR fragments as described in Material and Methods and are schematically shown in Fig. 3. All generated chimeric HeLa transfectants were tested by Northern blot hybridization (*data not shown*), immunofluorescence analyses (Fig. 1) and microinjection of neurobiotin (Table 1) for function. In this way, the HeLa transfectant of each chimeric construct that showed the strongest

Table 1. Transfer of tracer molecules and electrical conductances of homotypic gap junctions

Cell type	Neurobiotin (number of colored cells)	Lucifer yellow (number of colored cells)	Gap junction conductance, $g_{j,max}$ (nS)
Wild-type	2.2 ± 1.5	0.4 ± 0.7	<0.04 $n = 3$
Cx26	177 ± 12*	19.9 ± 3.0*	6.3 ± 1.8; $n = 8$
Cx26*30C2	162 ± 11*	7.7 ± 2.1*	9.1 ± 1.4; $n = 5$
Cx26*30C3	150 ± 10*	12.5 ± 2.5*	3.9 ± 1.4; $n = 5$
Cx26*30C2,C3	149 ± 10*	0.4 ± 0.8	3.1 ± 0.5; $n = 6$
Cx30	166 ± 12*	0.3 ± 0.6	3.7 ± 0.7; $n = 17$
Cx30*26C2	149 ± 9*	0.3 ± 0.6	9.1 ± 0.7; $n = 4$
Cx30*26C3	175 ± 12*	0.4 ± 0.8	11.2 ± 1.0; $n = 4$
Cx30*26C2,C3	179 ± 10*	10.8 ± 2.3*	8.5 ± 1.7; $n = 5$

The transfer data represent means of ± SD of $n > 20$; *n:* number of experiments; *: significance at $P < 0.001$ (Student's *t*-test). The conductance data are means ± SEM.

Table 2. Functionality of heterotypic combinations of HeLa Cx26 and -30 transfectants with other HeLa connexin transfectants

Connexin	Combinations	
	Functional	Nonfunctional
26	26*, 30, 32*, 46*, 50*	wt, 30.3*, 31*, 31.1*, 37*, 40*, 43*, 45*, 57
30	26, **30, 30.3,** 32, **40, 43, 45,** 46, 50	wt, 31, 31.1, 37, 57

Functionality was tested by assaying neurobiotin transfer between transfectants. Combinations that are functional with Cx30 but are nonfunctional with Cx26 are indicated by bold numbers.
* Results reported by Elfgang et al. (1995), shown here for comparison.
wt, nontransfected (wild-type) HeLa cells.

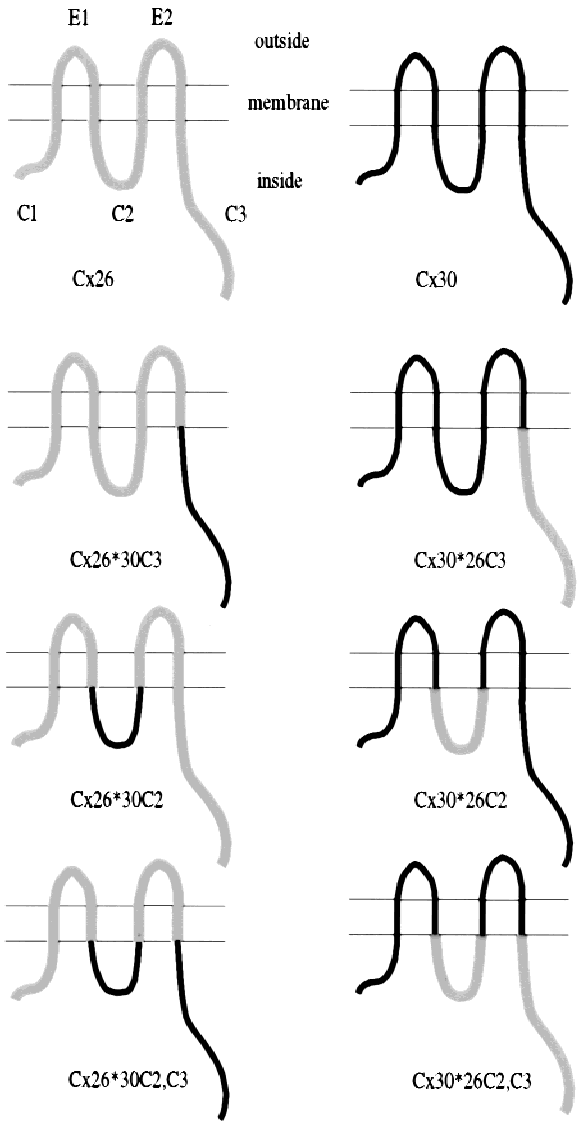

Fig. 3. Schematic representation and nomenclature of chimeric constructs obtained by exchanging presumptive domain sequences of Cx26 (grey) and Cx30 (black).

RNA hybridization signal of the expected molecular weight and the highest efficiency of neurobiotin transfer, was selected for further analyses. The results of neurobiotin and Lucifer yellow transfer in the selected chimeric and parental HeLa connexin transfectants are listed in Table 1. All HeLa transfectants showed homotypic neurobiotin transfer and, therefore, functional gap junction channels. Five min after Lucifer yellow injection (standard evaluation time), dye transfer was readily seen in Cx26 wild type transfectants, in the chimeric transfectants Cx26∗30C2, Cx26∗30C3 and, surprisingly, in Cx30∗26C2,C3 cells. No homotypic Lucifer yellow transfer in the other chimeric HeLa transfectants was detected during this time.

Electrical Properties of Chimeric Gap Junction Channels

HeLa cells expressing chimeric connexins were also used to determine the extent of intercellular coupling with the dual voltage-clamp method. For this purpose, we utilized normally coupled cell pairs forming homotypic gap junctions. Small voltage pulses of short duration (amplitude: 10 mV; duration: 0.5 to 1 sec) were applied repetitively to one cell of a cell pair to establish a junctional voltage, V_j, and measure the junctional current, I_j. This protocol prevented interference from V_j-dependent inactivation of I_j and hence enabled us to determine the maximal conductance, $g_{j,\max}$. The data obtained are summarized in Table 1. It also contains $g_{j,\max}$ data previously gained from pairs of wild-type HeLa cells (Valiunas et al., 2000) and transfected HeLa cells forming homotypic Cx26 and Cx30 gap junction channels (Bukauskas and Weingart, unpublished; Valiunas et al., 1999a). In transfected cells, $g_{j,\max}$ was at least 60 to 230 times larger than in wild-type cells. On average $g_{j,\max}$ varied 3.4-fold or less among different transfectants. A comparison of electrical and diffusional data yielded no obvious correlation. Hence, the absence of Lucifer yellow diffusion in some transfectants is unlikely to be caused by decreased connexin expression.

Prompted by the diffusion studies, the constructs Cx26∗30C2,C3 and Cx30∗26C2,C3 were then chosen to examine in more detail the electrical properties of homotypic gap junctions and gap junction channels. These clones exemplify the divergent diffusional behavior. Construct Cx26∗30C2,C3 allowed the intercellular diffusion of neurobiotin, but not of Lucifer yellow, construct Cx30∗26C2,C3 enabled the permeation of both. In a series of experiments we used pairs of cells whose gap junctions consisted of many channels. They were appropriate to assess the properties of gap junctions.

Figure 4 shows junctional current records, I_j, from a Cx26∗30C2,C3 cell pair (trace *a*) and a Cx30∗26C2,C3 cell pair (trace *b*) of comparable $g_{j,\max}$. The currents were elicited by the same bipolar pulse (±100 mV, 5 sec/5 sec), starting from a common holding potential, $V_1 = V_2 = -40$ mV. Hyperpolarization of cell 1 of a cell pair gave rise to an outward current in cell 2 which decayed with time to reach a quasi-steady level, depolarization gave rise to an inward current with the same properties. Both events indicate that I_j inactivation was faster and more complete in the case of the Cx30∗26C2,C3 cell pair.

Figure 5*A* summarizes the results from 5 complete experiments of this kind with cells expressing Cx30∗26C2,C3. It shows the relationship between the gap junction conductance, g_j, and the transjunctional voltage, V_j. The data depicted were gained as follows. V_j gradients of long duration (4 to 60 sec), different amplitude (up to 100 mV) and either polarity were ad-

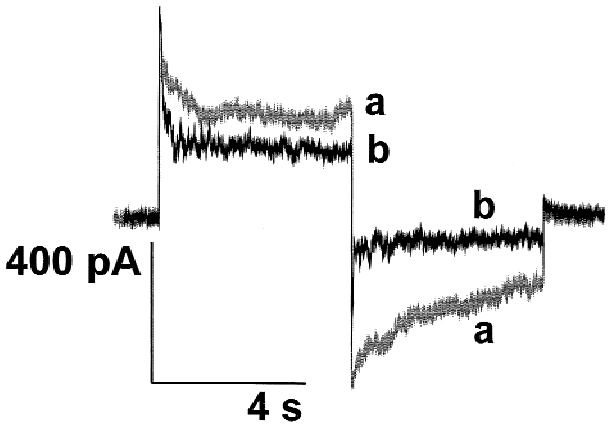

Fig. 4. Superimposed gap junction currents, I_j, recorded from a cell pair consisting of Cx26∗30C2,C3 transfectants (*a;* grey trace *a*) and a cell pair consisting of Cx30∗26C2,C3 transfectants (*b;* black trace *b*). Currents were elicited by biphasic pulses starting with a hyperpolarization followed by a depolarization (±100 mV). I_j inactivation was faster and more complete in the case of Cx30∗26C2,C3 cells.

ministered to cell 1 of a cell pair while I_j was recorded from cell 2. For analysis, the amplitude of I_j was determined at the beginning ($I_{j,\text{inst}}$; inst: instantaneous) and end ($I_{j,ss}$; ss: steady state) of each V_j pulse to calculate the conductances $g_{j,\text{inst}} = I_{j,\text{inst}}/V_j$ and $g_{j,ss} = I_{j,ss}/V_j$. The values of $g_{j,ss}$ were normalized with respect to $g_{j,\text{inst}}$ and plotted versus V_j. Each symbol corresponds to a single determination, each type of symbol refers to a cell pair. The smooth curve represents the best fit of data to the Boltzmann equation. The analysis yielded the following parameters: $V_{j,0} = 59$ mV, $g_{j,\min} = 0.2$, $z = 2.5$. $V_{j,0}$ is the voltage at which $g_{j,ss}$ is half-maximally inactivated, $g_{j,\min}$ is the normalized minimal conductance at large V_j and z is the equivalent number of unitary charges moving through the electric field applied. The data yielded a bell-shaped relationship which was nearly symmetrical.

Figure 5*B* summarizes the results from 6 complete experiments with cells expressing Cx26∗30C2,C3. With increasing V_j, the normalized values of $g_{j,ss}$ decreased in a symmetrical manner. However, $g_{j,ss}$ did not settle for a minimum even at the largest voltage successfully tested, i.e. $V_j = \pm 130$ mV (the cells did not tolerate larger voltages). The smooth curve represents the best fit of data to the Boltzmann equation for following parameters: $V_{j,0} = 109$ mV, $g_{j,\min} = 0$ $z = 0.5$. A $g_{j,\min}$ declining to zero may be real or reflect missing data at large voltages (*see* e.g., Valiunas et al., 1999b). With regard to the latter possibility, an independent estimate of $g_{j,\min}$ can be obtained from the ratio of the single channel conductances, i.e. $\gamma_{j,\text{residual}}/\gamma_{j,\text{main}}$ (*see* e.g. Valiunas et al., 1999a). Based on the channel data presented below, $g_{j,\min}$ would be 0.21. Using this value in the analysis of data in Fig. 5*B*, $V_{j,0}$ turns out to be 102 mV.

In another series of experiments, we used cell pairs

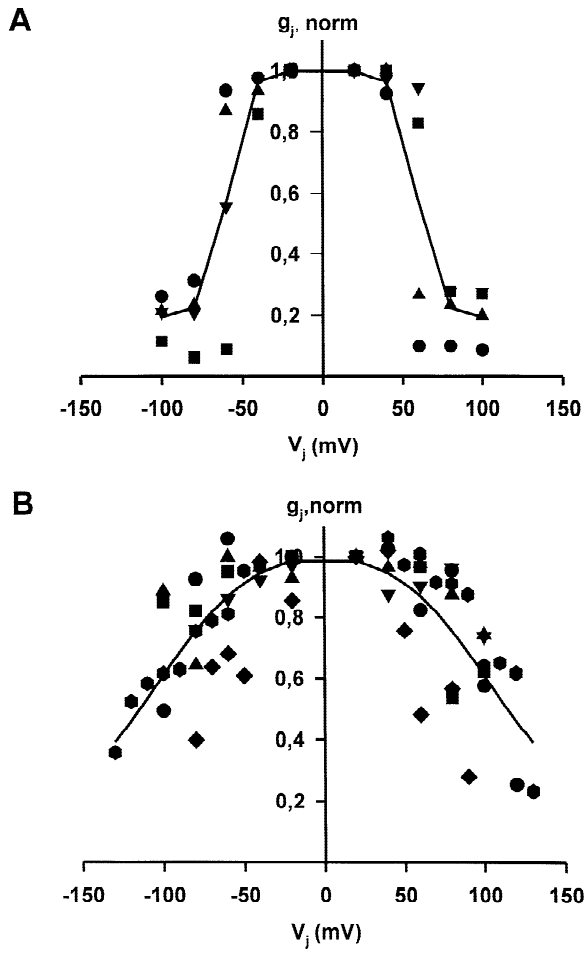

Fig. 5. Dependence of gap junction conductance, $g_{j,\text{norm}}$, on transjunctional voltage, V_j. Each symbol represents a single determination. Different symbols refer to different cell pairs. Smooth curves reflect the best fit of data to the Boltzmann equation. (*A*) Homotypic Cx30∗36C2,C3 gap junction. $V_{j,0} = 59$ mV, $g_{j,\min} = 0.2$, $z = 2.5$ ($n = 5$). (*B*) Homotypic Cx26∗30C2,C3 gap junction. $V_{j,0} = 109$ mV, $g_{j,\min} = 0$, z = 0.5 ($n = 6$).

whose gap junctions consisted of few channels only. These preparations were suitable to assess the properties of single channels. Figure 6*A* illustrates records obtained with this approach from cells expressing Cx30∗26C2,C3. A voltage pulse of 60 mV amplitude and 3 sec duration (dots mark interruption of traces due to acquisition) was applied to cell 1 (upper trace) of a cell pair while the associated current I_j was recorded from cell 2 (lower trace; channel opening: downward deflection). The current signal exhibited rapid transitions involving at least three levels corresponding to the main open state (lower level), the residual state (upper level) and a substate in between. Prior and after the pulse, I_j was at the reference current level that was different from the residual current level. The analysis yielded the following conductances: $\gamma_{j,\text{main}} = 134$ pS, $\gamma_{j,\text{residual}} = 15$ pS, $\gamma_{j,\text{substate}} = 94$ pS.

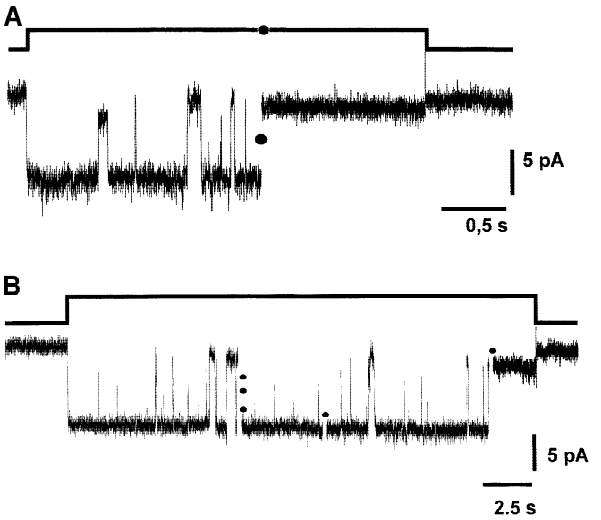

Fig. 6. Single gap junction channel currents. The transjunctional voltage, V_j, was 60 mV. The dots mark interruptions of traces due to data acquisition. (*A*) Homotypic Cx30∗26C2,C3 gap junction channel. (*B*) Homotypic Cx26∗30C2,C3 gap junction channel.

Using all-point histograms from current records (50 transitions or more) obtained from 6 cell pairs, we obtained the following values: $\gamma_{j,\text{main}} = 130 \pm 5$ pS, $\gamma_{j,\text{residual}} = 26 \pm 4$ pS. Hence, the ratio $\gamma_{j,\text{residual}}/\gamma_{j,\text{main}}$ equals 0.2, i.e. it is identical to $g_{j,\text{min}}$ determined from multichannel currents (*see* above). This finding is consistent with the current concept of gap junction channel operation (cf. Bruzzone et al., 1996).

Figure 6*B* illustrates records gained from a cell pair expressing Cx26∗30C2,C3. The voltage V_j established was 60 mV and lasted 40 sec (dots mark interruption of traces). The accompanying I_j showed transitions between the main open state and the residual state. In between, there were short hints of substates. The analysis of the current record led to a $\gamma_{j,\text{main}}$ of 133 pS and a $\gamma_{j,\text{residual}}$ of 36 pS. Summarizing the data from 7 cell pairs (all-point histograms from records with at least 50 current transitions), we obtained the following values: $\gamma_{j,\text{main}} = 146 \pm 8$ pS, $\gamma_{j,\text{residual}} = 30 \pm 4$ pS. Thus, the ratio $\gamma_{j,\text{residual}}/\gamma_{j,\text{main}}$ works out as 0.21. At $V_j = 60$ mV, Cx30∗26C2,C3 channels (cf. Fig. 6*B*) showed a higher incidence of transitions between the main state and residual state than Cx26∗30C2,C3 channels (compare Figs. 6*A* and *B*). Hence, the latter stayed preferentially in the main state.

Discussion

Since Cx30 is most closely related in its amino acid sequence to Cx26, we have examined the similarity of these genes and their protein products in more detail. First, we found that the two genes are closely linked on the proximal region of mouse chromosome 14. Together with the high nucleotide sequence identity, this finding further underlines the close evolutionary relationship of these genes. Functional studies then revealed that mouse Cx30 expressed in human HeLa cells, in contrast to HeLa-Cx26 transfectants, does not show cell-to-cell transfer of Lucifer yellow, although both transfectants exhibit transfer of neurobiotin and similar gap junction conductances.

Furthermore, we studied the heterotypic coupling between Cx30 hemichannels and other connexin hemichannels by microinjection of neurobiotin and compared the results with the heterotypic coupling of Cx26 hemichannels as reported by Elfgang et al. (1995). We found further differences between these gap junction channels of high sequence identity: Cx26 and Cx30 form functional heterotypic channels with the same connexins of the β-connexin subgroup, but Cx30 hemichannels in addition form functional channels with Cx30.3, Cx40, Cx43 and Cx45, i.e., with members of the α-connexin subgroup (cf. Table 2). Zhu et al. (1998) have reported the identification of critical amino acid residues in the E2 domain that determine the docking specificity of heterotypic interactions between connexins of the α- and β-subfamily. Thus, amino acid differences between E2 of Cx26 and Cx30 may be responsible for the observed differences in heterotypic coupling.

The analysis of homotypic dye transfer also revealed differences. The gap junction channels between Cx30 transfectants were not permeable to Lucifer yellow. When the results of Lucifer yellow transfer were compared with those of neurobiotin transfer in Cx26 and Cx30 transfectants (Fig. 2 and Table 1), it became evident that the difference is not due to a lower expression of Cx30 channels. This conclusion is consistent with the measurements of $g_{j,\text{max}}$. Hence, we hypothesized that the different diffusion of Lucifer yellow through Cx30 and Cx26 channels is caused by differences in the amino acid sequence of the C2 and/or C3 regions of these connexins. To test this hypothesis, we constructed chimeric Cx26/30 molecules by exchanging one or both of these domains and expressed the constructs in HeLa cells. Examining the chimerae with a Cx30 backbone, we found that both C2 and C3 from Cx26 have to be present to restore the Lucifer yellow transfer. Studying chimerae with a Cx26 backbone, we observed that the presence of either C2 or C3 from Cx26 is sufficient to maintain Lucifer yellow transfer, albeit at a lower level than in Cx26 transfectants. Lucifer yellow transfer only ceased when both C2 and C3 of Cx26 were absent. This suggests that C2 and C3 of Cx30 act as filtering devices for transjunctional diffusion of solutes. Discrimination may occur on the basis of size and/or charge of a solute. Considering the properties of Lucifer yellow (molecular mass 443 Da; minimal dimension 9.5 Å; two negative charges) and

neurobiotin (molecular mass 287 Da; minimal dimension 5.4 Å; one positive charge), we suggest that C2 and C3 of Cx30 may discriminate by forming an appropriate access funnel. If one takes into account the neurobiotin data, differences in the extent of Lucifer yellow transfer can be interpreted as follows. On the one hand, the decrease in Lucifer yellow transfer from parental Cx26 channels to the chimeric Cx26-channels Cx26∗30C2 and Cx26∗30C3 reflects molecular sieving by C2 and C3 of Cx30. On the other hand, the decrease in Lucifer yellow transfer from parental Cx26 channels to the chimeric Cx30 channels Cx30∗26C2,C3 indicates discrimination by the backbone of the Cx30 proteins forming the channel pore. Since Cx30∗26C2,C3 channels have a larger $\gamma_{j,\text{main}}$ than Cx26 channels (*see* below), this suggests that the Cx30 pore region impairs the transfer of negatively charged solutes.

How do the changes in diffusional properties of the channels, caused by the structural modifications of the connexins, correlate with the changes in electrical properties? To answer this question, electrophysiological measurements were performed using chimerae that revealed the most dramatic changes in the dye transfer studies when compared with HeLa cells expressing parental Cx26 and Cx30 channels, i.e., the constructs Cx26∗30C2,C3 and Cx30∗26C2,C3. These chimeric channels yielded unitary conductances of 146 and 130 pS, respectively. These values are intermediate between those previously reported for parental Cx26 and Cx30 channels, i.e., 102 and 179 pS (Valiunas et al., 1999a; Valiunas et al., 1999b). Hence, the exchange of C2 and C3 between Cx26 and Cx30 caused a decrease in unitary conductance when the domains replaced originated from Cx26, and an increase when the domains were from Cx30. This suggests a direct effect of C2 and C3 on channel conductance brought about by structural changes at the channel mouth, the domains of Cx26 and Cx30 decreasing and increasing, respectively, the unitary conductance. Alternatively, they could reflect indirect effects due to secondary changes in the region of the channel lumen. A comparison of the observed changes in unitary conductance and the changes in dye transfer leads to the following picture. On the one hand, substitution of C2 and C3 in Cx26 impaired the Lucifer yellow transfer, but increased $\gamma_{j,\text{main}}$. On the other hand, substitution of C2 and C3 in Cx30 improved the Lucifer yellow transfer, but decreased $\gamma_{j,\text{main}}$. This puzzle may be resolved if one considers the ionic selectivity of the channels. Unfortunately, this approach is excluded because relevant data are currently available for Cx26 channels only; they favour cations over anions (Suchyna et al., 1999). Moreover, it should be kept in mind that electrical and diffusional properties do not necessarily match up (cf. Bruzzone et al., 1996).

The exchange of C2 and C3 between Cx26 and Cx30 gave rise to a different pattern of changes in voltage sensitivity of the gap junction channels. Substitution of C2 and C3 in Cx26 provoked an increase in $V_{j,0}$ from 94 mV (Valiunas et al., 1999b) to 103 or 109 mV, depending on whether we assume a $g_{j,\text{min}}$ of 0.21 or 0, respectively (*see* Electrical Properties of Chimeric Gap Junction Channels). Substitution of C2 and C3 in Cx30 led to an increase in $V_{j,0}$ from 27 mV (Valiunas et al., 1999b) to 59 mV. Therefore, swapping of C2 and C3 reduces the voltage sensitivity of V_j-gating in both constructs examined. This indicates that the C2 and C3 domains of Cx26 and Cx30 exert a negative cumulative effect on the voltage sensitivity of V_j-gating of the backbone of the channel proteins, either directly or indirectly. Therefore, the V_j-sensitivity of Cx26 and Cx30 channels is modified, but not exclusively determined by the domains C2 and C3 of the connexins. This conclusion is consistent with recent data gained from Cx32 and Cx43 segment mutations (Barrio, Castro & Gomez-Hernandez, 1999). Recently it has been reported that charge substitution in C1 of Cx26 and Cx32 affects the polarity of V_j-gating (Oh et al., 1999). This is another indication that intracellular domains of connexins are involved in V_j-gating.

The comparison of single channel and multichannel records discloses an apparent paradox. Cx30∗26C2,C3 cells exhibited a $\gamma_{j,\text{residual}}$ and a $g_{j,\text{min}} \neq 0$ while Cx26∗30C2,C3 cells showed a $\gamma_{j,\text{residual}}$ and a $g_{j,\text{min}} \cong 0$. The former properties resemble the behavior of homotypic Cx30 channels and are consistent with the notion that $g_{j,\text{min}}$ reflects the existence of $\gamma_{j,\text{residual}}$ (Valiunas et al., 1999a). The latter properties may reflect the limited range of V_j tolerated by the Cx26∗30C2,C3 cells ($\leq$130 mV) in conjunction with their large $V_{j,0}$ (109 mV). In this context, it is interesting to note that homotypic Cx26 channels rarely exhibit residual states, i.e., they flicker primarily between the main state and closed state, and show a $g_{j,\text{min}} \neq 0$ (Valiunas et al., 1999b; *see* also Bukauskas and Weingart, 1995). In the present study, we observed no fast current transitions involving the closed state. Conceivably, this state may be the result of a unique structural combination involving the pore and mouth region of Cx26 channels. Recently, it has been shown that mutations in the Cx30 gene cause nonsyndromic autosomal dominant deafness in humans (Grifa et al., 1999), similar as defects in the human Cx26 gene (Kelsell et al., 1997; Denoyelle et al., 1997). Since Cx30 and Cx26 are both expressed in the cochlea, possibly in the same cells (Lautermann et al., 1998), functional differences and possible interactions between these connexin channels are likely to be clinically relevant.

This work was supported by grants of the Deutsche Forschungsgemeinschaft (SFB 284, project C1), the Thyssen Stiftung and the Fonds der Chemischen Industrie (to K.W.), the Swiss National Science Founda-

tion (31-55297.98 to R.W.) and the Bundesamt für Bildung und Wissenschaft (95.0824-2 to R.W.).

References

Adamson, M.C., Silver, J., Kozak, C.A. 1991. The mouse homologue of the gibbon ape leukemia virus receptor: genetic mapping and a possible receptor function in rodents. *Virology* **183:**778–781

Barrio, L.C., Castro, C., Gomez-Hernandez, J.M. 1999. Altered assembly of gap junction channels caused by COOH-terminal connexin32 mutants of CMTX. *Ann. N.Y. Acad. Sci.* **883:**526–529

Bennett, M.V.L. 1997. Gap junctions as electrical synapses. *J. Neurocytol.* **26:**339–366

Beyer, E.C., Goodenough, D.A., Paul, D.L. 1988. The connexins, a family of related gap junction proteins. *In:* Gap Junctions. E.L. Hertzberg, R.G. Johnson, editors. pp. 167–175. A.R. Liss, New York

Bruzzone, R., White, T.W., Paul, D.L. 1996. Connections with connexins: the molecular basis of direct intercellular signaling. *Eur. J. Biochem.* **238:**1–27

Bukauskas, F.F., Weingart, R. 1995. Heterotypic gap junction channels (connexin26-connexin32) violate the paradigm of unitary conductance. *Pfluegers Arch.* **429:**870–872

Cao, F., Eckert, R., Elfgang, C., Nitsche, J.M., Snyder, S.A., Hülser, D.F., Willecke, K., Nicholson, B.J. 1998. A quantitative analysis of connexin-specific permeability differences of gap junctions expressed in HeLa transfectants and *Xenopus* oocytes. *J. Cell Sci.* **111:**31–43

Condorelli, D.F., Parenti, R., Spinella, F., Trovarto Salinaro, A., Belluardo, N., Cardile, V., Cicirata, F. 1998. Cloning of a new gap junction gene (Cx36) highly expressed in mammalian brain neurons. *Eur. J. Neurosci.* **10:**1202–1208

Dahl, E., Winterhager, E., Reuss, B., Traub, O., Butterweck, A., Willecke, K. 1996a. Expression of the gap junction proteins connexin31 and connexin43 correlates with communication compartments in extraembryonic tissues and in the gastrulating mouse embryo, respectively. *J. Cell Sci.* **109:**191–197

Dahl, E., Manthey, D., Chen, Y., Schwarz, H.J., Chang, Y.S., Lalley, P.A., Nicholson, B.J., Willecke, K. 1996b. Molecular cloning and functional expression of mouse connexin-30, a gap junction gene highly expressed in adult brain and skin. *J. Biol. Chem.* **271:**17903–17910

Davies, T.C., Barr, K.J., Jones, D.H., Zhu, D.G., Kidder, G.M. 1996. Multiple members of the connexin gene family participate in preimplantation development of the mouse. *Dev. Genet.* **18:**234–243

Delmar, M., Stergiopoulous, K., Homma, N., Ek-Vitorin, J.F., Taffet, S.M. 1998. A Ball-and-Chain Model for the Chemical Regulation of Connexin43. *In:* Gap Junctions. R. Werner, editor. pp. 8–12. IOS Press, Washington

Delorme, B., Dahl, E., Jarry-Guichard, T., Briand, J.P., Willecke, K., Gros, D., Théveniau-Ruissy, M. 1997. Expression pattern of connexin gene products at the early developmental stages of the mouse cardiovascular system. *Circ. Res.* **81:**423–437

Denoyelle, F. et al. 1997. Prelingual deafness: high prevalence of a 30delG mutation in the connexin 26 gene. *Hum. Mol. Genet.* **6:**2173–2177

Dermietzel, R., Leibstein, A., Frixen, U., Janssen-Timmen, U., Traub, O., Willecke, K. 1984. Gap junctions in several tissues share antigenic determinants with liver gap junctions. *EMBO J.* **3:**2261–2270

Eckert, R., Dunina-Barkovskaya, A., Hülser, D.F. 1993. Biophysical characterization of gap junction channels in HeLa cells. *Pfluegers Arch.* **205:**404–407

Elfgang, C., Eckert, R., Lichtenberg-Fraté, H., Butterweck, A., Traub, O., Klein, R.A., Hülser, D.F., Willecke, K. 1995. Specific permeability and selective formation of gap junction channels in connexin-transfected HeLa cells. *J. Cell Biol.* **129:**805–817

Gimlich, R.L., Kumar, N.M., Gilula, N.B. 1990. Differential regulation of the levels of three gap junction mRNAs in *Xenopus* embryos. *J. Cell Biol.* **110:**597–605

Goldberg, G.S., Bechberger, J.F., Naus, C.C.G. 1995. A pre-loading method of evaluating gap junctional communication by fluorescent dye transfer. *BioTechniques* **18:**490–497

Goodenough, D.A., Goliger, J.A., Paul, D.L. 1996. Connexins, connexons, and intercellular communication. *Ann. Rev. Biochem.* **65:**475–502

Graham, F.L., van der Eb, A.J. 1973. A new technique for the assay of infectivity of human adenovirus 5 DNA. *Virology* **52:**456–459

Grifa, A., Wagner, C.A., D'Ambrosio, L., Melchionda, S., Bernardi, F., Lopez-Bigas, N., Rabionet, R., Arbones, M., Della Monica, M., Estivill, X., Zelante, L., Lang, F., Gasparini, P. 1999. Mutations in GJB6 cause nonsyndromic autosomal dominant deafness at DFNA3 locus. *Nature Genetics* **23:**16–18

Haefliger, J.A., Bruzzone, R., Jenkins, N.A., Gilbert, D.J., Copeland, N.G., Paul, D.L. 1992. Four novel members of the connexin family of gap junction proteins. Molecular cloning, expression and chromosome mapping. *J. Biol. Chem.* **267:**2057–2064

Haubrich, S., Schwarz, H.J., Bukauskas, F., Lichtenberg-Frate, H., Traub, O., Weingart, R., Willecke, K. 1996. Incompatibility of connexin 40 and 43 hemichannels in gap junctions between mammalian cells is determined by intracellular domains. *Mol. Biol. Cell* **7:**1995–2006

Hennemann, H., Kozjek, G., Dahl, E., Nicholson, B.J., Willecke, K. 1992. Molecular cloning of mouse connexins26 and -32: similar genomic organization but distinct promoter sequences of two gap junction genes. *Eur. J. Cell Biol.* **58:**81–89

Horst, M., Harth, N., Hasilik, H. 1991. Biosynthesis of glycosylated human lysozyme mutants. *J. Biol. Chem.* **266:**13914–13919

Hoshi, T., Zagotta, W.N., Aldrich, R.W. 1990. Biophysical and molecular mechanisms of Shaker potassium channel inactivation. *Science* **250:**533–538

Kelsell, D.P., Dunlop, J., Stevens, H.P., Lench, N. J., Liang, J.N., Parry, G., Mueller, R.F., Leigh, I.M. 1997. Connexin 26 mutations in hereditary non-syndromic sensorineural deafness. *Nature* **387:**80–83

Kozak, C.A., Peyser, M., Krall, M., Mariano, T.M., Kumar, C.S., Pestka, S., Mock, B.A. 1990. Molecular genetic markers spanning mouse chromosome 10. *Genomics* **8:**519–524

Kozak, C.A., Dymecki, S.M., Niederhuber, J.E., Desiderio, S.V. 1991. Genetic mapping of the gene for a novel tyrosine kinase, BLK, to mouse chromosome 14. *Genomics* **9:**762–764

Kunzelmann, P., Schröder, W., Traub, O., Steinhäuser, C., Dermietzel, R., Willecke, K. 1999. Late onset and increasing expression of the gap junction protein connexin 30 in adult murine brain and long term cultured astrocytes. *Glia* **25:**111–119

Laird, D.W., Revel, J.P. 1990. Biochemical and immunochemical analysis of the arrangement of connexin43 in rat heart gap junction membranes. *J. Cell Sci.* **97:**109–117

Lautermann, J., ten Carte, W.-J., Altenhoff, P., Grümmer, R., Traub, O., Frank, H.-G., Jahnke, K., Winterhager, E. 1998. Expression of the gap-junction connexins26 and 30 in the rat cochlea. *Cell Tissue Res.* **294:**415–420

Manthey, D., Bukauskas, F., Lee, C.G., Kozak, C.A., Willecke, K. 1999. Molecular Cloning and Functional Expression of the Mouse Gap Junction Gene Connexin57 in Human HeLa Cells. *J. Biol. Chem.* **274:**14716–14723

Marten I., Hoshi, T. 1997. Voltage-dependent gating characteristics of

the K^+ channel KAT1 depend on the N and C termini. *Proc. Natl. Acad. Sci. USA* **94:**3448–3453

Milks, L.J., Kumar, N.M., Houghten, R., Unwin, N., Gilula, N.B. 1988. Topology of the 32-kd liver gap junction protein determined by site-directed antibody localizations. *EMBO J.* **7:**2967–2975

Miyazaki, S., Kozak, C.A., Marchetti, A., Buttitta, F., Gallahan, D., Callahan, R. 1995. The chromosomal location of the mouse mammary tumor gene Int6 and related pseudogenes in the mouse genome. *Genomics* **27:**420–424

Nadarajah, B., Jones, A.M., Evans, W.H., Parnavelas, J.G. 1997. Differential expression of connexins during neocortical development and neuronal circuit formation. *J. Neurosci.* **17:**3096–3111

Oh, S., Rubin, J.B., Bennett, M.V.L., Verselis, V.K., Bargiello, T.A. 1999. Molecular determinants of electrical rectification of single channel conductance in gap junctions formed by connexins 26 and 32. *J. Gen. Physiol.* **114:**339–364

Sambrook, J., Fritsch, E.F., Maniatis, T. 1989. Molecular cloning: a laboratory manual. Cold Spring Harbor Press, New York

Schwarz, H.J., Chang, S., Hennemann, H., Dahl, E., Lalley, P.A., Willecke, K. 1992. Chromosomal assignments of mouse connexin genes, coding for gap junctional proteins, by somatic cell hybridization. *Somat. Cell. Mol. Genetics* **18:**351–359

Simon, A.M., Goodenough, D.A. 1998. Diverse functions of vertebrate gap junctions. *Trends Cell Biol.* **8:**477–483

Söhl, G., Degen, J., Teubner, B., Willecke, K. 1998. The murine gap junction gene connexin36 is highly expressed in mouse retina and regulated during brain development. *FEBS Letters* **428:**27–31

Strata, F., Atzori, M., Molnar, M., Ugolini, G., Berretta, N., Cherubini, E. 1998. Nitric oxide sensitive depolarization-induced hyperpolarization: a possible role for gap junctions during development. *Eur. J. Neurosci.* **10:**397–403

Suchyna, T.M., Nitsche, J.M., Chilton, M., Harris, A.L., Veenstra, R.D., Nicholson, B.J. 1999. Different ionic selectivities for connexin 26 and 32 produce rectifying gap junction channels. *Biophys. J.* **77:**2968–2987

Teubner, B., Odermatt, B., Güldenagel, M., Söhl, G., Degen, J., Bukauskas, F.F., Kronengold, J., Verselis, V.K., Jung, Y.T., Kozak, C.A., Schilling, K., and Willecke, K. 2001. Functional expression of the new gap junction gene connexin47 transcribed in mouse brain and spinal cord neurons. *J. Neuroscience* **214:**1117–1126

Temme, A., Buchmann, A., Gabriel, H.D., Nelles, E., Schwarz, M., Willecke, K. 1997. High incidence of spontaneous and chemically induced liver tumors in mice deficient for connexin32. *Curr. Biol.* **7:**713–716

Traub, O., Look, J., Dermietzel, R., Brümmer, F., Hülser, D., Willecke, K. 1989. Comparative characterization of the 21-kD and 26-kD gap junction proteins in murine liver and cultured hepatocytes. *J. Cell Biol.* **108:**1039–1051

Valiunas, V., Manthey, D., Vogel, R., Willecke, K., Weingart, R. 1999a. Biophysical properties of mouse connexin30 gap junction channels studied in transfected HeLa cells. *J. Physiol.* **519:**631–644

Valiunas, V., Niessen, H., Willecke, K., Weingart, R. 1999b. Electrophysiological properties of gap junction channels in hepatocytes isolated from connexin32-deficient and wild-type mice. *Pfluegers Arch.* **437:**846–856

Valiunas, V., Weingart, R., Brink, P.R. 2000. Formation of heterotypic gap junction channels by connexins 40 and 43. *Circ. Res.* **86:**e42–e49

Willecke, K., Hennemann, H., Dahl, E., Jungbluth, S., Heynkes, R. 1991. The diversity of connexin genes encoding gap junctional proteins. *Eur. J. Cell Biol.* **56:**1–7

Yamasaki, H., Naus, C.C. 1996. Role of connexin genes in growth control. *Carcinogen.* **17:**1199–1213

Zhang, J.T., Nicholson, B.J. 1994. The topological structure of connexin 26 and its distribution compared to connexin 32 in hepatic gap junctions. *J. Membrane Biol.* **139:**15–29

Zhu, H., Cinbotaru, M., Nicholson, B.J. 1998. The residues determine docking specificity of heterotypic interactions between connexins of different subfamilies. *Mol. Biol. Cell* **9:**94a